Annals of Botany **125**: 805–819, 2020
doi: 10.1093/aob/mcz160, available online at www.academic.oup.com/aob

ANNALS OF BOTANY
Founded 1887

PART OF THE FOCUS ISSUE ON PLANT DEFENCE AND STRESS REPSONSE

The *SAUR41* subfamily of *SMALL AUXIN UP RNA* genes is abscisic acid inducible to modulate cell expansion and salt tolerance in *Arabidopsis thaliana* seedlings

Ting Qiu, Mengyuan Qi, Xiaohui Ding, Yanyan Zheng, Tianjiao Zhou, Yong Chen, Ning Han, Muyuan Zhu, Hongwu Bian and Junhui Wang*

Institute of Genetics and Regenerative Biology, College of Life Sciences, Zhejiang University, Hangzhou 310058, China
** For correspondence. E-mail junhuiwang@zju.edu.cn*

Received: 24 April 2019 Returned for revision: 9 June 2019 Editorial decision: 25 September 2019 Accepted: 2 October 2019
Published electronically 5 October 2019

• **Background and Aims** Most primary auxin response genes are classified into three families: *AUX/IAA*, *GH3* and *SAUR* genes. Few studies have been conducted on *Arabidopsis thaliana SAUR* genes, possibly due to genetic redundancy among different subfamily members. Data mining on arabidopsis transcriptional profiles indicates that the *SAUR41* subfamily members of *SMALL AUXIN UP RNA* genes are, strikingly, induced by an inhibitory phytohormone, abscisic acid (ABA). We aimed to reveal the physiological roles of arabidopsis *SAUR41* subfamily genes containing *SAUR40*, *SAUR41*, *SAUR71* and *SAUR72*.
• **Methods** Transcriptional responses of arabidopsis *SAUR41* genes to phytohormones were determined by quantitative real-time PCR. Knock out of *SAUR41* genes was carried out with the CRISPR/Cas9 (clustered regulatory interspaced short palindromic repeats/CRISPR-associated protein 9) genome editing technique. The *saur41/40/71/72* quadruple mutants, *SAUR41* overexpression lines and the wild type were subjected to ultrastructural observation, transcriptome analysis and physiological characterization.
• **Key Results** Transcription of arabidopsis *SAUR41* subfamily genes is activated by ABA but not by gibberellic acids and brassinosteroids. Quadruple mutations in *saur41/40/71/72* led to reduced cell expansion/elongation in cotyledons and hypocotyls, opposite to the overexpression of *SAUR41*; however, an irregular arrangement of cell size and shape was observed in both cases. The quadruple mutants had increased transcription of calcium homeostasis/signalling genes in seedling shoots, and the *SAUR41* overexpression lines had decreased transcription of iron homeostasis genes in roots and increased ABA biosynthesis in shoots. Notably, both the quadruple mutants and the *SAUR41* overexpression lines were hypersensitive to salt stress during seedling establishment, whereas specific expression of *SAUR41* under the ABA-responsive *RD29A* (*Responsive to Desiccation 29A*) promoter in the quadruple mutants rescued the inhibitory effect of salt stress.
• **Conclusions** The *SAUR41* subfamily genes of arabidopsis are ABA inducible to modulate cell expansion, ion homeostasis and salt tolerance. Our work may provide new candidate genes for improvement of plant abiotic stress tolerance.

Key Words: *Arabidopsis thaliana*, *SMALL AUXIN UP RNA* genes, abscisic acid, cell expansion, ion homeostasis, salt tolerance, CRISPR/Cas9, transcription profiling.

INTRODUCTION

During plant growth and development, the phytohormone auxin modulates cell division, differentiation and elongation, largely by regulating gene expression. Most of the primary auxin response genes are classified into three families: *AUXIN/INDOLE-3-ACETIC ACID* (*AUX/IAA*), *GRETCHENHAGEN3* (*GH3*) and *SMALL AUXIN UP RNA* (*SAUR*) (Hagen and Guilfoyle, 2002). While great progress has been made in our understanding of the molecular mechanisms of both AUX/IAAs and GH3s, functional studies on SAURs have lagged behind, and have only begun to be performed in recent years (reviewed in Ren and Gray, 2015; Stortenbeker and Bemer, 2018).

SAUR genes are the largest family of primary auxin response genes, with plant SAUR proteins being divided into three families (Stortenbeker and Bemer, 2018), and arabidopsis SAURs phylogenetically classified into three clades (Kodaira *et al.*, 2011). *SAUR* genes are regulated at both transcriptional and post-transcriptional levels in response to multiple hormonal and environmental signals (reviewed in Ren and Gray, 2015; Stortenbeker and Bemer, 2018). Some transcription factors that regulate the expression of arabidopsis *SAUR* genes have been identified. For example, the arabidopsis Cys2/His2 zinc-finger proteins AZF1 and AZF2 repress many clade I and clade II *SAUR* genes under salt stress and abscisic acid (ABA) treatment (Kodaira *et al.*, 2011). Similarly, the MADS-domain factor FRUITFULL represses *SAUR10* in stems and inflorescence branches to control arabidopsis growth and architecture (Bemer *et al.*, 2017). SOB3 (SUPPRESSOR OF PHYTOCHROME B4-#3) and BZR1 (BRASSINAZOLE RESISTANT 1) inactivate and activate, respectively, the transcription of *SAUR19*

genes to modulate hypocotyl growth in response to auxin and brassinosteroid (BR) signalling (Favero *et al.*, 2017), while PIF3 (PHYTOCHROME INTERACTING FACTOR 3) and TCP4 (TEOSINETE BRANCHED1, CYCLOIDEA and PCF) antagonistically regulate *SAUR16/50* during de-etiolation of arabidopsis cotyledons (Sun *et al.*, 2016; Dong *et al.*, 2019).

The SAUR proteins are diverse in their subcellular localizations and undergo complex post-translational control (reviewed in Ren and Gray, 2015). Based on results from overexpression studies, many arabidopsis SAUR proteins have been revealed to promote cell expansion, including SAUR19s (Franklin *et al.*, 2011; Spartz *et al.*, 2012), SAUR63s (Chae *et al.*, 2012), SAUR41 (Kong *et al.*, 2013), SAUR36 (Stamm and Kumar, 2013), SAUR76–78 (Li *et al.*, 2015), SAUR14/50/65 (Sun *et al.*, 2016) and SAUR10s (van Mourik *et al.*, 2017). In addition, it has been demonstrated that SAUR36 functions as a positive regulator of leaf senescence (Hou *et al.*, 2013), SAUR76 functions as a cell division regulator (Markakis *et al.*, 2013) and an ethylene receptor modulator (Li *et al.*, 2015), while SAUR62/75 are required for pollen tube growth (He *et al.*, 2018). Functional studies on the SAURs of other plant species are very limited. It has been reported that rice (*Oryza sativa*) OsSAUR39 (Kant *et al.*, 2009) and OsSAUR45 (Xu *et al.*, 2017) serve as negative regulators of auxin biosynthesis/transportation, cassava (*Manihot esculenta*) MeSAUR1 functions as a transcriptional regulator of the gene encoding the small subunit of ADP-glucose pyrophosphorylase (Ma *et al.*, 2017), wheat (*Triticum aestivum*) TaSAUR75 positively regulates drought and salt stress (Guo *et al.*, 2017), and tomato (*Solanum lycopersicum*) SlSAUR69 is involved in the unripe-to-ripe phase transition of tomato fruit (Shin *et al.*, 2018).

The mechanisms by which arabidopsis SAURs mediate cell expansion are of great interest, but remain largely unknown. It has been suggested that arabidopsis peripheral membrane SAUR19s inhibit several members of the PP2C.D-type protein phosphatases to increase Thr947 phosphorylation of plasma membrane H^+-ATPases, resulting in apoplast acidification and cell expansion (Spartz *et al.*, 2014). Arabidopsis SAUR19 constitutively expressed in *S. lycopersicum* also inhibited endogenous PP2C.Ds to confer auxin-independent hypocotyl elongation (Spartz *et al.*, 2017). Further support for an antagonistic role for PP2C.D proteins against SAUR-mediated cell expansion comes from a study on loss-of-function mutants of the plasma membrane-localized sub-set of arabidopsis PP2C.Ds (Ren *et al.*, 2018). Thus, SAURs and PP2C.Ds may be novel components for the acid growth theory that links auxin to the cell expansion process (reviewed in Haruta *et al.*, 2015; Arsuffi and Braybrook, 2017). As an alternative mechanism, a recent study suggests that SAUR62/75 interact with ribosomal protein RPL12 family members to promote ribosome assembly and protein translation required for pollen tube growth (He *et al.*, 2018).

Alongside auxin, the phytohormone ABA regulates many aspects of plant growth and development such as seed germination, cotyledon greening/expansion, stomatal closure, drought resistance and salt resistance. The core ABA signalling network is well understood (reviewed in Cutler *et al.*, 2010; Hubbard *et al.*, 2010). Briefly, ABA binds to intercellular Pyrabactin Resistance/Regulatory Component of ABA Receptor (PYR/RCAR) receptors to inhibit the PP2C.A type protein phosphatases, which leads to release of SNF1-Related Protein Kinase 2 (SnRK2) family members; these activate ion channels, transcription factors and other targets (Hauser *et al.*, 2017). Identification of new components capable of modulating ABA sensitivity/response is of great value for engineering plant abiotic stress tolerance.

Many auxin-responsive genes, including most *SAUR* genes in clades I and II, were found to be commonly downregulated to establish growth inhibition and growth adaptation under abiotic stress conditions and ABA treatment (Kodaira *et al.*, 2011). However, based on microarray and transcriptome data, the expression of the arabidopsis *SAUR41* subfamily genes (*SAUR40*, *SAUR41*, *SAUR71* and *SAUR72*), attributed to clade III, is strikingly induced by the growth-inhibiting hormone ABA, unlike most other *SAUR* genes (Leonhardt *et al.*, 2004; Kodaira *et al.*, 2011; Zeng *et al.*, 2012; reviewed in Ren and Gray, 2015). This raises the question of whether the balanced expression of ABA-repressed and ABA-induced *SAUR* genes is necessary for abiotic responses. In addition, we found that *SAUR41* genes have tissue-specific and developmentally regulated expression patterns during arabidopsis seedling establishment. *SAUR41* was distinctively expressed in the quiescent centre and cortex/endodermis initials of root stem cell niches and in the endodermis of hypocotyls (Kong *et al.*, 2013), whereas *SAUR71* and *SAUR72* were expressed in the steles of young roots and hypocotyls; in addition, *SAUR71* was differentially expressed during stomatal development (Qiu *et al.*, 2013). Taken together, further studies on *SAUR41* genes may be helpful to reveal new interactions between auxin and ABA or new players in plant abiotic responses. An essential prerequisite for understanding the physiological roles of *SAUR41* genes is the generation of loss-of-function mutants. In recent years, the development of CRISPR/Cas9 (clustered regularly interspaced short palindromic repeats/CRISPR-associated protein 9) genome editing techniques for arabidopsis makes it possible to generate high orders of mutants for genes of interest very efficiently (Fauser *et al.*, 2014).

Here, we verify that arabidopsis *SAUR41* genes were activated by ABA. Knockout of all *SAUR41* subfamily members using the CRISPR/Cas9 system led to reduced cell expansion in young arabidopsis seedlings. The quadruple mutants increased the transcription of multiple calcium homeostasis/signalling genes in seedling shoots, while the *SAUR41* overexpression lines decreased the transcription of iron homeostasis genes in roots and increased ABA biosynthesis in shoots. However, both the quadruple mutants and *SAUR41* overexpression were hypersensitive to salt treatment. Notably, specific expression of *SAUR41* under an ABA-responsive promoter in quadruple mutants rescued the inhibitory effect of salt on seedling establishment and growth. We suggest that the *SAUR41* subfamily genes of arabidopsis are new players in modulation of cell expansion, ion homeostasis and salt tolerance to fine-tune seedling growth. Our work also indicates that balanced expression of ABA-repressed and ABA-induced SAURs may be necessary for plant abiotic responses.

MATERIALS AND METHODS

Plant material and growth conditions

Arabidopsis thaliana ecotype Columbia-0 (Col-0) were used as sources of wild-type plant material. Seeds were surface-sterilized and sown aseptically on 9 cm Petri dishes containing Gamborg's B5 medium with 1 % (w/v) sucrose and 0.8 or 1.0

% (w/v) agar, for horizontal and vertical growth, respectively. The basal salts and vitamins of B5 medium were composed of (mg L^{-1}): KNO_3 2500, $CaCl_2{\cdot}2H_2O$ 150, $MgSO_4{\cdot}7H_2O$ 250, $(NH_4)_2SO_4$ 134, $NaH_2PO_4{\cdot}H_2O$ 150, KI 0.75, H_3BO_3 3.0, $MnSO_4{\cdot}H_2O$ 10, $ZnSO_4{\cdot}7H_2O$ 2.0, $Na_2MoO_4{\cdot}2H_2O$ 0.25, $CuSO_4{\cdot}5H_2O$ 0.025, $CoCl_2{\cdot}6H_2O$ 0.025, $FeSO_4{\cdot}7H_2O$ 27.8, Na_2-EDTA 37.3, myo-inositol 100, nicotinic acid 1.0, pyridoxine HCl 1.0, and thiamine HCl 10. The plates were maintained at 4 °C for 2–3 d, then transferred to a culture room (23 °C; 30–40 % relative humidity; 80 µmol m^{-2} s^{-1} irradiance with a 16 h photoperiod).

Design of guide RNAs for CRISPR/Cas9 genomic editing

SAUR41 subfamily genes were knocked out using the CRISPR/Cas9 genome editing technique developed for arabidopsis (Fauser *et al.*, 2014). The choice of target site motif, $(N)_{20}$NGG, was based on the online tool ZIFIT Target Version 4.2 (http://zifit.partners.org/ZiFiT/Introduction.aspx). We selected three target sites for each gene. The DNA targets and the corresponding guide RNA are illustrated in Supplementary data Fig. S1.

Expression vector construction and plant transformation

Expression vectors were constructed using the GATEWAY™ cloning system (Invitrogen, Carlsbad, CA, USA). Entry vectors containing sequences of interest were created first in the pENTR™ backbone, and then they were incubated together with the corresponding destination vectors to generate the expression vectors via the LR recombination reaction (Karimi *et al.*, 2002; She *et al.*, 2010). For CRISPR/Cas9 genome editing, we used the Golden Gate cloning strategy (Engler *et al.*, 2009) and two rounds of PCR to create entry clones encoding guide RNAs. Primers used for amplification of the *U6-26* promoter and guide RNA coding sequences are listed in Supplementary data Table S1. Each entry vector was confirmed by DNA sequencing. To generate final expression vectors, the destination vector pDe-CAS9-ccdB (Fauser *et al.*, 2014) was employed. For overexpression of *SAUR41* genes, entry clones were created first, and suitable destination vectors for overexpression of fusion proteins were used as described previously (Kong *et al.*, 2013; Qiu *et al.*, 2013). For expression of *SAUR41-EGFP* from the *RD29A* promoter, the original *Cauliflower mosaic virus* (CaMV) *35S* promoter in the protein localization construct *35S::SAUR41-EGFP* (Kong *et al.*, 2013) was replaced with a *ccdB* fragment including the *attR1* and *attR2* sites by a previously described method (Yang *et al.*, 2012). Briefly, the *ccdB* fragment was PCR-amplified using *pH7FWG2,0* as a template, with the primers *ccdB-Up* and *ccdB-Dn*, containing an introduced *Hin*dIII and *Spe*I site, respectively. The *ccdB* fragment was then digested to replace the *35S* promoter sequence, thus forming the destination vector *ccdB-SAUR41-EGFP* for promoter-specific expression. PCR primers used for construction of the *RD29A* entry vector and the *ccdB-SAUR41-EGFP* destination vector are listed in Supplementary data Table S1. All expression vectors were electroporated into *Agrobacterium tumefaciens* strain GV3101, and plants were transformed using the vacuum infiltration method (Bechtold, 1993). Transgenic plants were selected on B5 plates with 12.5 µg mL^{-1} hygromycin or 10 µg mL^{-1} Basta depending on the selectable marker genes.

Mutation detection and plant crossing

For genome editing, DNA mutations in the leaves of the T_1 primary transformants and in the young seedlings of T_2 and T_3 generations were detected by T7E1 endonuclease digestion or PAGE analysis. Primers for detection of CRISPR/Cas9-induced mutations in *SAUR41* genes are listed in Supplementary data Table S1. Germline mutations were identified through Sanger sequencing of PCR products spanning the target sites. We first achieved single mutants for each gene of the *SAUR41* subfamily, then created double, triple and quadruple mutants by crossing and screening. Briefly, gene-specific primers, listed in Supplementary data Table S1 were used in the PCR-based screen by genotyping the individual F_2 progeny plants of each cross.

Tissue sections and microscopy

For transmission electron microscopy (TEM), hypocotyls of 6-day-old seedlings were cut into 0.5–1.0 cm pieces, vacuum-infiltrated and then fixed in 2.5 % glutaraldehyde overnight, followed by treatment with 1 % osmium tetroxide for 2 h. Specimens were then dehydrated with a graded series of ethanol solutions and embedded in Spurr resin. Micro-thin (1 µm) and ultra-thin (70–90 nm) sections were prepared with a LEICA EM UC7 ultratome. Micro-sections were stained with 0.1 % methylene blue in 0.1 M phosphate-buffered saline solution for 2 min at 60 °C and then washed with distilled water. Micro-sections were visualized and imaged by a Nikon Eclipse 80i microscope. Ultra-thin sections were stained with 2 % uranyl acetate in 50 % ethanol for 15 min and then with 0.3 % alkaline lead citrate (pH 12, adjusted by NaOH) for 30 min (Yang *et al.*, 2012). Ultra-thin sections were imaged with a Hitachi Model H-7650 TEM.

RNA isolation, quantitative real-time PCR (qRT-PCR) and transcriptome analysis

For transcriptional response of *SAUR41* genes to the treatments with various plant hormones, 5-day-old arabidopsis seedlings were transferred into liquid B5 medium containing 10 µM naphthaleneacetic acid (NAA), ABA or gibberellic acid (GA_3), and incubated on a rotary shaker (50 rpm) for 0.5, 1.0, 2.0, 3.0 and 4.0 h. The treatments were conducted during the middle part of the light period. Control seedlings were treated with an equivalent volume of dimethylsulphoxide (DMSO), the solvent for the phytohormone stock solutions.

For RNA isolation, whole or different parts of arabidopsis seedlings were frozen and ground to powder in liquid nitrogen, followed by total RNA extraction using TRizol reagent (Takara Bio Inc., Kusatsu, Shiga, Japan). Extracted RNA was treated with RNase-free DNase I (Takara) and subjected to first-strand

cDNA synthesis using AMV reverse transcriptase (Takara). The qRT-PCR was performed on the Mastercycler Realplex System (Eppendorf, Hamburg, Germany) using SYBR Green reagent (Takara). Relative mRNA levels were normalized using *Ubiquitin Extension Protein 1* (*UBQ1*) as the standard (Yang *et al.*, 2012). Primers for qRT-PCR measurement of *SAUR41* subfamily genes, validation of RNA sequencing (RNA-seq) results and expression assay of salt tolerance genes are listed in Supplementary data Table S1.

For transcriptional profiling (RNA-seq), total RNA samples were sent to Vazyme Biotech Co., Ltd (Nanjing, China) for the following processes: library construction; Illumina HiSeq sequencing; and bioinformatics analysis, including a quality check of the raw reads, alignment of raw reads to the arabidopsis genome, assembly of gene expression from aligned reads and identification of differential gene expression, followed by Gene Ontology (GO), KEGG pathway and gene/protein network analysis. Each sample generated 4 Gb of clean data and contained three biological replicates. These data have been deposited in the Gene Expression Omnibus (GEO) at NCBI (National Center for Biotechnology Information, https://www.ncbi.nlm.nih.gov/geo/) with accession numbers GSE134117 and GSE134119.

Determination of ABA and metal iron contents

The ABA concentration in 7-day-old seedlings was measured using a method modified from Pan *et al.* (2010). Tissue (0.2 g) was frozen and ground to powder in liquid nitrogen, then dissolved in a buffer containing isopropanol, hydrochloric acid and distilled water (2:0.002:1, v/v/v). Extracts were shaken at 4 °C for 30 min followed by addition of 20 mL of dichloromethane. The final extracts were dissolved in methanol containing 0.1 % methane acid. The level of ABA was determined by high-performance liquid chromatography–tandem mass spectrometry (HPLC-MS/MS). Reversed-phase HPLC was performed with a ZORBAX SB-C18 column (2.1 × 150 mm; 3.5 µm; Agilent Technologies, Santa Clara, CA, USA). The mobile phase A was 0.1 % (v/v) formic acid in distilled water, while the mobile phase B was 0.1 % (v/v) formic acid in methanol. The flow rate was 0.6 mL min^{-1} at 40 °C and the injection volume was 10 µL. ABA was quantified with a SCIEX-6500 Qtrap mass spectrometer (Applied Biosystems, Foster City, CA, USA) connected online to the output of the HPLC column.

Iron, calcium, sodium and potassium concentrations in 7-day-old seedlings were measured using a method described by Wild *et al.* (2016). Tissues were digested completely in a nitric acid–hydrogen peroxide solution (2:1, v/v) before inductively coupled plasma-atomic emission spectrometry (ICP-AES) on an Agilent 710 ICP-AES spectrometer (Agilent Technologies): power output, 1000 W; plasma gas rate, 15.0 L min^{-1}; atomizer pressure, 200 kPa; auxiliary gas rate, 1.5 L min^{-1}; pump speed, 15 rpm.

Growth measurement, salt tolerance, statistical analysis and image processing

Plates containing arabidopsis seedlings were digitally photographed after 5–12 d of incubation. Hypocotyl length, root length, cotyledon petiole length and cotyledon size were measured from magnified images using ImageJ software. The cell lengths of epidermal cells and cortical cells of hypocotyls were measured as described by Kong *et al.* (2013). Rhizosphere acidification was visualized by a method described by Spartz *et al.* (2014). For the salt tolerance assay, 100 and 150 mM NaCl were applied at the time of seed imbibition at 4 °C for 2 d. The seedling establishment rate was scored after 7 d of germination and growth at 23 °C. A seedling was regarded as established when the radicle was at least 5 mm long and the cotyledon was open and green (Thomas *et al.*, 1995). The fresh weight (f. wt) of seedlings was recorded at the same time. Growth inhibition was calculated as (f. wt under salt stress – f.wt in control conditions)/f. wt in control conditions × 100 %. Each treatment contained approx. 30 seedlings or approx. 90 seeds and was replicated three times. Statistical analyses were performed using Microsoft Excel and Student's *t*-test. Images were processed using Adobe Photoshop CC.

RESULTS

The SAUR41 subfamily genes are induced by ABA but not by GA and BR

Using promoter reporter lines, we found that members of the *SAUR41* subfamily had tissue-specific and developmentally regulated expression patterns in young arabidopsis seedlings (Kong *et al.*, 2013; Qiu *et al.*, 2013). In hypocotyls, *SAUR41* was predominantly expressed in the endodermis, while *SAUR71* and *SAUR72* were mainly expressed in pericycles; in roots, *SAUR41* was expressed in stem cell niches and the endodermis, *SAUR71* were expressed in pericycles, while *SAUR72* was expressed in both the endodermis and pericycles (Kong *et al.*, 2013; Qiu *et al.*, 2013). In an arabidopsis *SAUR* gene expression pattern obtained from the Bio-Analytic Resource electronic Fluorescent Pictograph browser (BAR-eFP, http://bar.utoronto.ca/efp_arabidopsis/), *SAUR41* was predicted to be expressed in both shoots and roots; *SAUR71* was moderately expressed in shoots; *SAUR72* was highly active in roots; and data for *SAUR40* were unavailable (Kodaira *et al.*, 2011). Here, using qRT-PCR analysis, we found that the expression patterns of *SAUR41*, *SAUR71* and *SAUR72* were generally similar to the BAR-eFP prediction, with the slight difference that *SAUR71* was strongly expressed instead of moderately expressed in shoots (Fig. 1A, B). *SAUR40* was detectable in our qRT-PCR experiment: in the shoots/aerial parts of arabidopsis seedlings, it exhibited the lowest expression levels out of all four family members, but, in the roots, its transcription level was higher than that of *SAUR71* (Fig. 1A, B).

To determine plant hormone responses of *SAUR41* genes, 5-day-old light-grown seedlings were treated with 10 µM NAA, ABA or GA_3 for 0–4 h before qRT-PCR analysis. Results showed that, in the aerial parts, short-term NAA treatment increased the transcription levels of *SAUR40* and *SAUR41* by 2- to 3-fold; in contrast, the transcription levels of *SAUR19*, a well-documented auxin-responsive *SAUR* gene were increased by 23-fold (Fig. 2A). In the root parts, again, only *SAUR19* displayed a very rapid and dramatic NAA response (Fig. 2B). Treatment of arabidopsis seedlings with ABA increased the

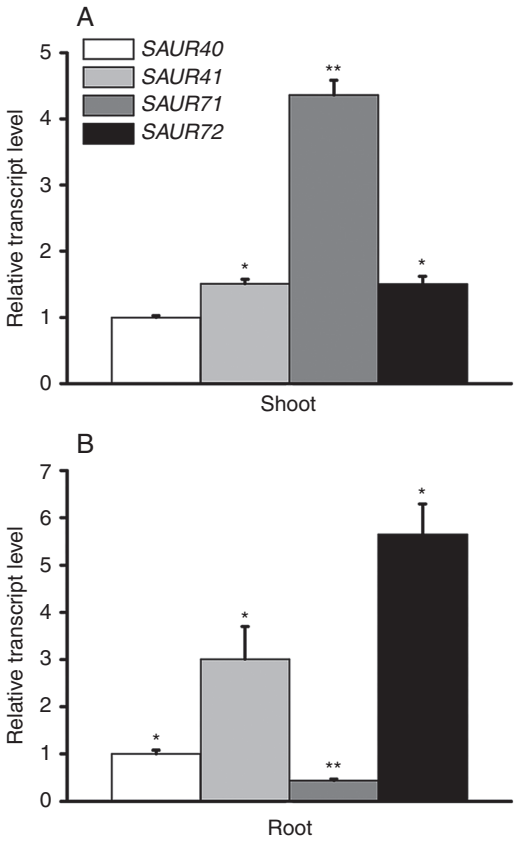

FIG. 1. Relative expression levels of *SAUR41* genes in 5-day-old arabidopsis seedlings. (A) Relative expression levels of *SAUR41* genes in seedling shoots. The transcript level of *SAUR40* is set to 1.0. *SAUR71* displays the highest expression level. (B) Relative expression levels of *SAUR41* genes in seedling roots. The transcript level of *SAUR40* is set to 1.0. *SAUR41* is expressed in both shoots and roots, while *SAUR72* is highly active in roots. Error bars represent the s.d. $^{**}P < 0.01$, $^{*}P < 0.05$, Student's *t*-test.

transcription levels of *SAUR41* genes by 3- to 5.5-fold in the aerial parts and by 2- to 3-fold in the root parts, while *SAUR19* was repressed by ABA treatment in both parts (Fig. 2C, D). Notably, *SAUR71* and *SAUR72* were especially ABA responsive in both shoots and roots, as compared with *SAUR40* and *SAUR41* (Fig. 2C, D). GA_3 treatment was unable to activate the expression of *SAUR41* genes (Fig. 2E, F), as was EBR (2,4-epibrassinolide) treatment (Supplementary data Fig. S2).

Generation of single, double, triple and quadruple mutants of the SAUR41 subfamily genes

To explore potential roles of *SAUR41* genes in arabidopsis development and physiology, we first screened T-DNA insertion lines from the Arabidopsis Biological Resource Center (ABRC). Line SALK_056969 contained a T-DNA at the promoter region of *SAUR41*, but this insertion did not impair its expression; in addition, line SALK_121397 was a false-positive line for the *SAUR41* gene (Kong *et al.*, 2013). For *SAUR40*, line SALK_040036 was annotated to contain a T-DNA at the intergenic region, and lines SALK_128948, SALK_051362 and SALK_050786 all contained T-DNA at the 5'-untranslated region. Similarly, no lines contained T-DNA insertions inside the coding regions of *SAUR71* and *SAUR72*. Thus, we used the CRISPR/Cas9 genome editing technique developed specifically for arabidopsis (Fauser *et al.*, 2014) to generate loss-of-function mutants for *SAUR 41* genes.

First, a set of single mutants was generated for each gene (Fig. 3). The impact of each mutation on the corresponding protein product was evaluated based on the integrity of the highly conserved approx. 60 amino acid SAUR domain (Ren and Gray, 2015). Mutations in *saur40* completely deleted the SAUR domain; mutations in *saur71* and *saur72* deleted a very large part of the SAUR domain; and mutations in *saur41-1* to *saur41-4* deleted one-third of the SAUR domain and the entire C-terminus, while the *saur41-5* mutation deleted the whole SAUR domain (Supplementary data Fig. S3). Subsequently, we crossed these single mutants and screened corresponding mutations to create double mutants, triple mutants and quadruple mutants. This allowed us to overcome potential functional redundancy among *SAUR41* subfamily members and also to eliminate potential off-target effects from the CRISPR/Cas9 technique.

In addition to the backcrosses, additional steps were taken to avoid potential off-target effects of the CRISPR/Cas9 technique. Transcriptome profiling studies (see below) provided both FPKM (fragments per kilobase of transcript sequence per millions base pairs sequenced) data as well as SNP (single nucleotide polymorphism) and InDel (insertion–deletion) data, which allowed us to confirm that there were no off-target knockouts of other *SAUR* genes during the mutation of *SAUR41* genes. Furthermore, software to predict potential off-target knockouts (CCTop, https://crispr.cos.uni-heidelberg.de/) determined that the *SAUR52* gene was the most likely candidate because it had only a 2 bp mismatch with the target of *SAUR72*. Using PAGE analysis, we did not detect any mutation in *SAUR52* during the mutations of *SAUR41* genes. From here on, the triple mutants *saur41-1saur71-1saur72-1*, *saur41-1saur40-1saur71-2* and *saur41-5saur40-1saur71-2* are abbreviated as *saur41/71/72*, *saur41/40/71*#1 and #2, while the quadruple mutants *saur41-1saur40-1saur71-1saur72-1*, *saur41-1saur40-1saur71-2saur72-1*, *saur41-5saur40-1saur71-1saur72-1* and *saur41-5saur40-1saur71-2saur72-1* are abbreviated as *saur41/40/71/72*#1 to #4, respectively.

Inactivation of SAUR41 subfamily genes leads to reduced and disordered cell expansion

To characterize phenotypes of *saur41* mutants, we first performed morphological analysis in comparison with the wild type and the *SAUR41* overexpression line (*35S::SAUR41-MYC* lines, abbreviated as *OE-SAUR41*; Kong *et al.*, 2013). In 7-day-old quadruple mutant seedlings, we found that the areas of cotyledons, and the lengths of hypocotyls and roots, were significantly reduced (Fig. 4A–D). The lengths of epidermal cells and cortical cells of hypocotyls were further measured across three genotypes, Col-0 (wild-type), *saur41/40/71/72* and *OE-SAUR41*. The results showed that cell length correlated

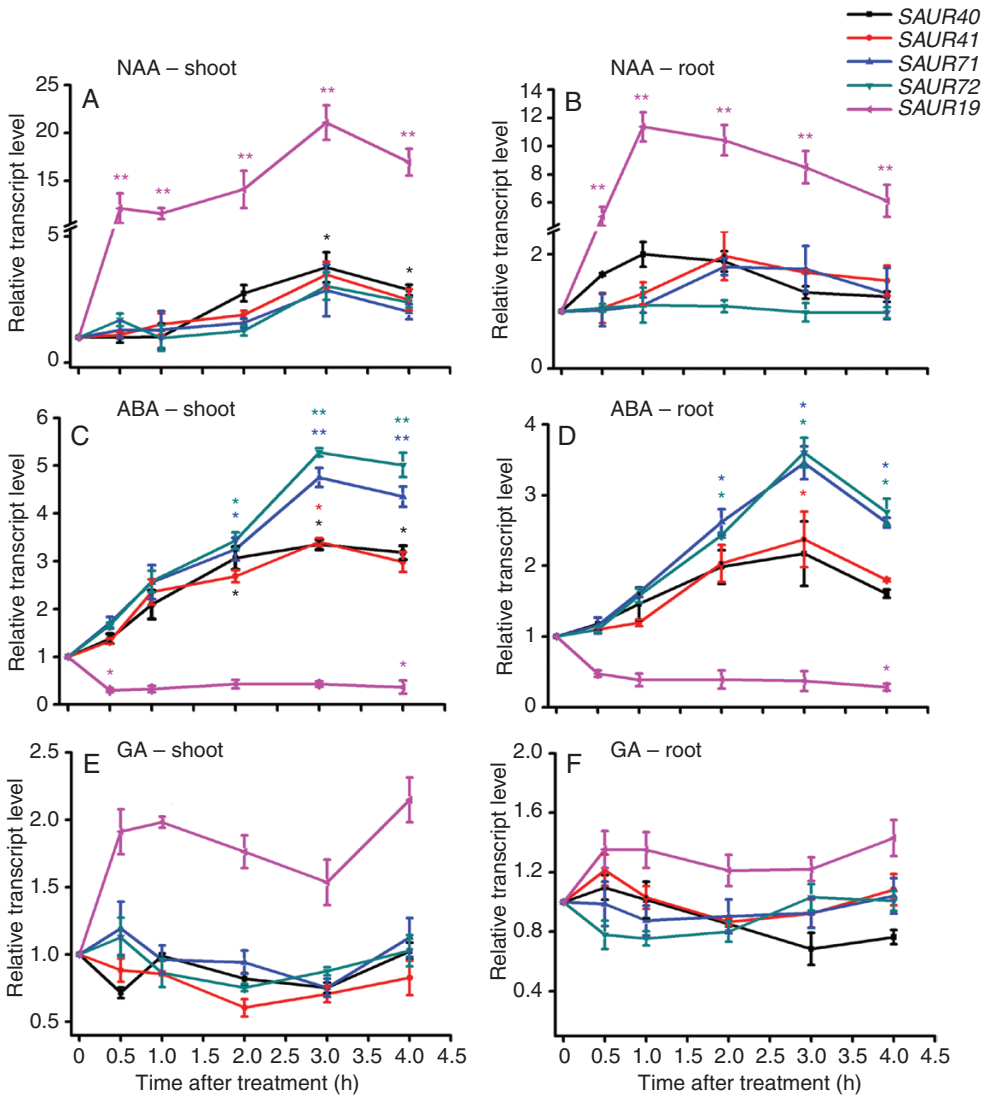

FIG. 2. The *SAUR41* subfamily genes are induced by ABA treatment. (A) Transcriptional responses of *SAUR41* genes and *SAUR19* to NAA treatment in seedling shoots. Five-day-old seedlings were incubated in liquid medium containing 10 μM NAA for 0.5, 1.0, 2.0, 3.0 and 4.0 h. *SAUR19* seems dramatically auxin responsive. (B) Transcriptional responses of *SAUR41* genes and *SAUR19* to NAA treatment in roots. (C) Transcriptional responses of *SAUR41* genes and *SAUR19* to ABA treatment in seedling shoots. Five-day-old seedlings were incubated in liquid medium containing 10 μM ABA for 0.5, 1.0, 2.0, 3.0 and 4.0 h. *SAUR19* is repressed by ABA, unlike *SAUR41* genes. (D) Transcriptional responses of *SAUR41* genes and *SAUR19* to ABA treatment in roots. Again, *SAUR41* genes are induced by ABA but *SAUR19* is repressed by ABA. (E) Transcriptional responses of *SAUR41* genes and *SAUR19* to GA treatment in seedling shoots. Five-day-old seedlings were incubated in liquid medium containing 10 μM GA for 0.5, 1.0, 2.0, 3.0 and 4.0 h. *SAUR19* is slightly induced by GA while *SAUR41* genes are not induced by GA. (F) Transcriptional responses of *SAUR41* genes and *SAUR19* to GA treatment in seedling roots. Each treatment contained three biological replicates. In all cases, the transcript levels of each gene without hormone treatment were set to 1.0. Error bars represent the s.d. $^{**}P < 0.01$, $^{*}P < 0.05$, Student's *t*-test.

with organ length (Fig. 4E), indicating that the short hypocotyl phenotype in quadruple mutants should be the result of a reduction in cell elongation. In 10-day-old quadruple mutant seedlings, the lengths of cotyledon petioles were also significantly reduced (Supplementary data Fig. S4).

Optical sections from the hypocotyls of 6-day-old seedlings revealed heterogeneous cell size in the endodermis of both the quadruple mutants and the *SAUR41* overexpression lines, with the shape of many endodermic cells changed from rectangular to circular ($n = 6$; Fig. 5A–F). Using TEM, we also found irregular arrangements of cell size and cell shape in the hypocotyl pericycles of *saur41/40/71/72* and *OE-SAUR41* ($n = 4$; Fig. 5G–I).

Quadruple mutants exhibit disordered transcription of calcium and ABA signalling genes

We used RNA-seq to profile differentially expressed genes in *saur41/40/71/72* mutants and *OE-SAUR41* overexpression lines as compared with the wild type. Shoot parts and root parts of 5-day-old seedlings were evaluated separately. Raw reads and processed data of RNA-seq experiments have been deposited in the GEO at NCBI. Information on differentially expressed genes including gene IDs, fold change and putative functions is given in Supplementary data Tables S2–S5. Venn diagrams (volcano plots) of wild-type shoot vs. mutant shoot, wild-type root vs. mutant root, wild-type shoot vs. overexpression shoot

FIG. 3. A set of single mutants for each *SAUR41* family member was generated by CRISPR/Cas9 genomic editing. Protospacers (guide RNA targets) are marked in green and protospacer-adjacent motifs (PAMs) are marked in red. Heritable mutations were identified by Sanger sequencing.

and wild-type root vs. overexpression root were graphically illustrated, and it seemed that shoot samples had far more differentially expressed genes than root samples (Fig. 6A–D). Four corresponding histograms for GO analysis (enrichments of cellular components, molecular function and biological processes) have been included in Supplementary data Figs S5 and S6. Considering that *SAUR41* genes are induced by ABA (Fig. 2) to regulate cell expansion (Figs 4 and 5), among the significantly enriched biological processes, we chose certain gene sets related to ABA signalling/biosynthesis or ion homeostasis/signalling for qRT-PCR validation of gene transcription levels (Fig. 6E–H).

In the shoot parts of *saur41/40/71/72*, a set of calcium homeostasis/signalling genes were upregulated as compared with the wild type; these included *ACA1* (*Autoinhibited Ca^{2+}-ATPase 1*), *CML12/TOUCH3* (*Calmodulin-Like 12*), *CIPK9* (*CBL-Interacting Protein Kinase 9*), *CPK28* (*Calcium-Dependent Protein Kinase28*) and *CBP60F* (*Calmodulin-Binding Proteins 60F*) (Fig. 6E). In addition, a set of ABA signalling-related genes were differentially expressed in the shoot parts of the quadruple mutants: upregulated genes included *GBF3* (*G-box Binding Factor 3*), encoding a positive transcription factor for ABA signalling in branch bud control and dehydration response (Gonzalez-Grandio *et al.*, 2017; Ramegowda *et al.*, 2017), *ERD6* (*Early Response To Dehydration 6*), encoding a putative sucrose transporter, and *BKK1/SERK4* (*BRInsensitive1-Associated Kinase1-Like1/Somatic Embryogenesis Receptor-Like Kinase 4*), encoding a component for cross-talk between ABA and BR and for stomatal patterning (Meng *et al.*, 2015); downregulated genes included *RAV1* (*Related to ABA Insensitive3/Viviparous1*) and *TEM1* (*Tempranillo 1*), two negative transcription factor genes of ABA signalling (Feng *et al.*, 2014) (Fig. 6F).

Overexpression of SAUR41 decreases transcription of iron homeostasis genes in roots and increases transcription of ABA biosynthesis/signalling genes in shoots

In roots of the *SAUR41* overexpression seedlings, strikingly, of downregulated genes, approximately half were related to iron homeostasis; these included two transcription factor genes regulating the iron deficiency response (*ORG2/AtHLH38* and *ORG3/AtHLH39*) (Yuan *et al.*, 2008); iron transporter genes specific to the epidermis (*IRT1*) and phloem (*OPT3*), respectively; and a nicotianamine (NA) synthase gene (*NAS4*) that produces NA for the movement of iron via the NA–Fe complex (Fig. 6G).

In the shoot parts of the *SAUR41* overexpression seedlings, a set of genes related to ABA biosynthesis and signalling had significantly changed their transcription levels; these included *NCED3* (*Nine-Cis-Epoxycarotenoid Dioxygenase3*), a key gene for ABA biosynthesis which responds to leaf turgor decrease within minutes (Sussmilch *et al.*, 2017), *PYL7* (*Pyrabactin Resistance 1-Like 7/Regulatory Components Of ABA Receptor*), *HAI1* (*Highly ABA-Induced PP2C Family Clade A*), *AZF2* (*Arabidopsis Zinc Finger Transcription Factor*) and *AIB* (*ABA-Inducible bHLH-type Transcription Factor*) (Fig. 6H).

In light of the RNA-seq results, we measured metal ions (calcium, iron, sodium and potassium) and ABA contents in shoot parts of Col-0, *saur41/40/71/72* and *OE-SAUR41* seedlings. There were no differences on calcium content among the three

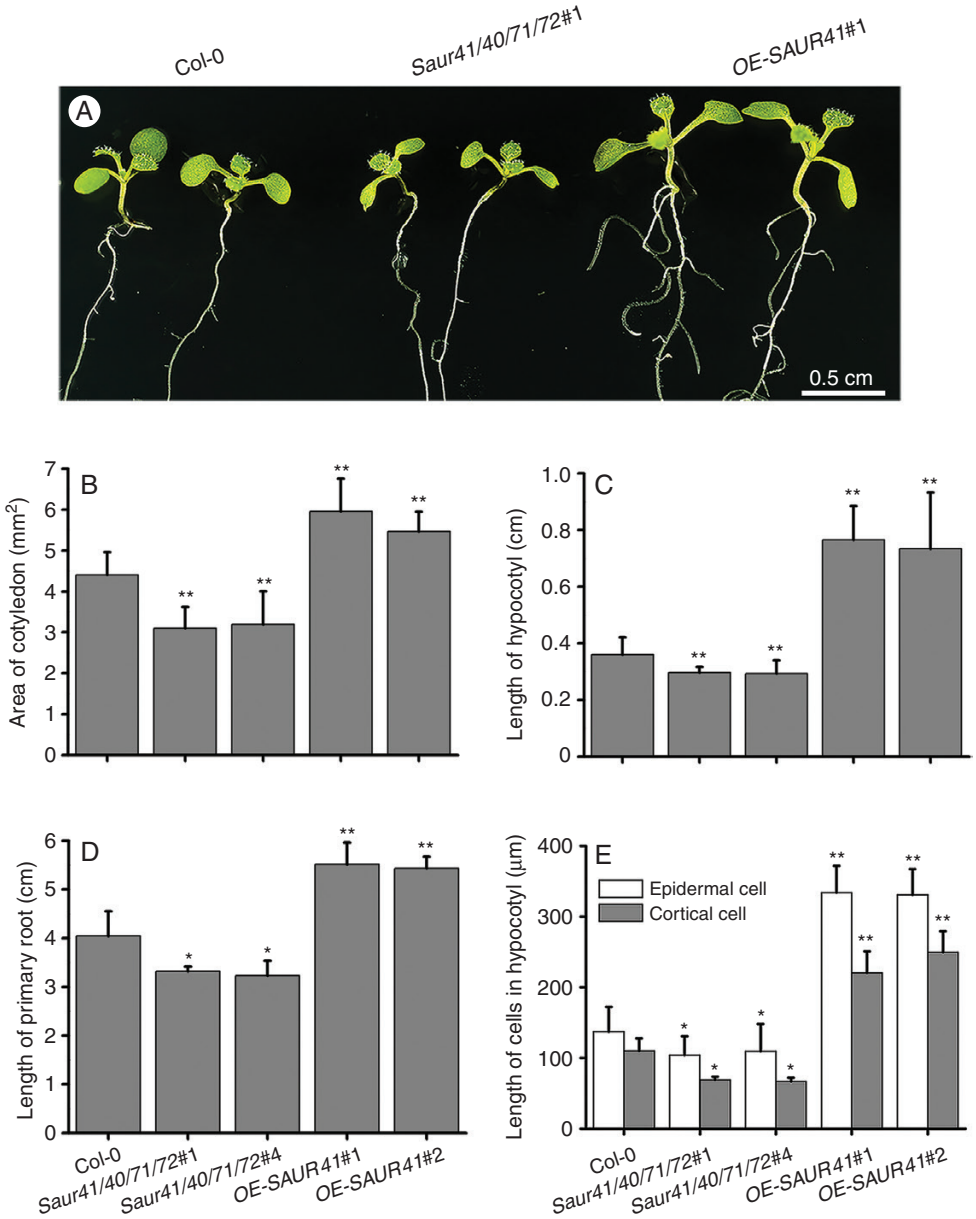

FIG. 4. Inactivation of *SAUR41* subfamily genes leads to reduced cell expansion. (A) Seven-day-old light-grown seedlings of the wild type, the *saur41* quadruple mutants *saur41/40/71/72* and the *SAUR41* overexpression lines *OE-SAUR41*. (B) Statistical comparison of cotyledon areas in 7-day-old seedlings of three genotypes. (C) Statistical comparison of hypocotyl length in 7-day-old seedlings. (D) Statistical comparison of root length in 7-day-old seedlings. (E) Statistical comparison of epidermal cell and cortical cell length in 7-day-old hypocotyls. The quadruple mutants *saur41-1sauir40-1saur71-1saur72-1* and *saur41-5sauir40-1saur71-2saur72-1* are abbreviated as *saur41/40/71/72*#1 and *saur41/40/71/72#4*, while the *35S::SAUR41-MYC* overexpression lines are abbreviated as *OE-SAUR41*#1 and #2. Each treatment contained approx. 30 seedlings or cells and was replicated three times. Error bars represent the s.d. $^{**}P < 0.01$, $^{*}P < 0.05$, Student's *t*-test.

genotypes (Fig. 7A), although calcium homeostasis/signalling genes were up-regulated in the quadruple mutants (Fig. 6E). This result indicated that the atomic emission spectrometry method used here to detect total calcium is unable to reveal the kinetic distribution of extracellular and cytosolic calcium. Interestingly, although the *OE-SAUR41* seedlings showed a reduced expression of iron homeostasis genes in roots (Fig. 6G), they contained higher amounts of iron in shoots (Fig. 7B), indicating that *SAUR41* overexpression may lead to an iron excess phenotype, resulting in a feedback effect. *OE-SAUR41* shoots accumulated much more potassium (Fig. 7C), while the quadruple mutants had reduced contents of sodium (Fig. 7D). The *OE-SAUR41* shoots showed increased expression of *NCED3* (Fig. 6H); as expected, these shoots contained higher amounts of ABA than the wild type and the quadruple mutants (Fig. 7E).

Both the quadruple mutants and the SAUR41 overexpression lines were hypersensitive to salt stress

As *SAUR41* genes are ABA inducible (Fig. 2) and both the quadruple mutants and the *SAUR41* overexpression lines exhibit

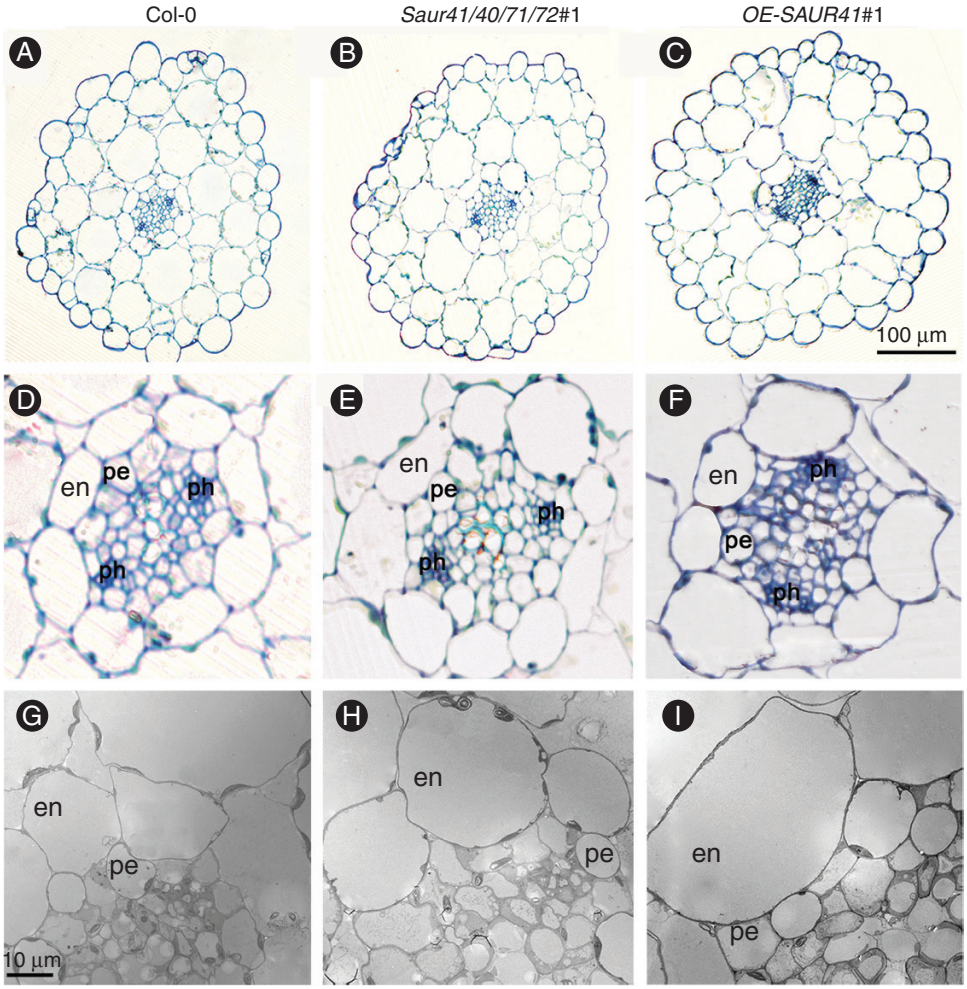

FIG. 5. Both inactivation of *SAUR41* genes and overexpression of *SAUR41* led to irregular arrangement of cell size and shape in endodermis and pericycles of arabidopsis hypocotyls. (A) Optical section of hypocotyls of 6-day-old wild-type (Col-0) seedlings. (B) Optical section of the quadruple mutants *saur41/40/71/72*. (C) Optical section of the *SAUR41* overexpression *OE-SAUR41* lines. (D) Enlargement of an optical section of the wild type. (E) Enlargement of an optical section of the quadruple mutant. (F) Enlargement of an optical section of the *SAUR41* overexpression line. (G) TEM of the wild type. (H) TEM of the quadruple mutant. (I) TEM of the *SAUR41* overexpression line. en, endodermis; pe, pericycle cells; ph, phloem.

altered expression of ABA biosynthesis and/or signalling genes (Fig. 6), we carried out abiotic stress response assays. After some primary investigations, we focused on salt stress in the present study. The results showed that both the quadruple mutants and the *SAUR41* overexpression lines were hypersensitive to 100 and 150 mM NaCl stresses as compared with the wild type (Fig. 8A). The overexpression lines in control conditions had the longest and overexpanded hypocotyls, so they had much higher biomass than Col-0 in control conditions. However, under NaCl stress, the overexpression lines appeared to be most affected: they had the lowest seedling establishment rate and the most significant fresh weight reduction (Fig. 8B, C). Notably, in the quadruple mutants, specific expression of *SAUR41* under the ABA-responsive *RD29A* (*Responsive to Desiccation 29A*) promoter rescued the inhibitory effect of salt on seedling establishment and growth (Fig. 8A–C). To carry out a rescue experiment for a quadruple mutant, the best approach is to introduce four transgenes into the mutant, but this will probably be quite difficult. As the *SAUR41* genes were ABA inducible, here we drove *SAUR41* expression by using the *RD29A* promoter (*RA29A::SAUR41*).

The transcription level and the stability of *SOS1* (*Salt Overly Sensitive* 1) mRNA, encoding an Na^+/H^+ antiporter and a salt tolerance determinant, are very sensitive to salt tress (Shi *et al.*, 2000; Deinlein *et al.*, 2014). For qRT-PCR assay of *SOS1* accumulation, 5-day-old seedlings were transferred into control medium or medium with 150 mM NaCl and grown for 2 d. The results showed that, under control conditions, the *SAUR41* overexpression lines had the highest expression of *SOS1*, but, under NaCl stress, they failed to increase the expression of *SOS1* further (Fig. 8D); this may one of the reasons why they were most sensitive to salt stress. The quadruple mutants were able to increase the expression of *SOS1* under salt stress (Fig. 8D), although they were salt sensitive as compared with the wild type (Fig. 8A–C).

Mechanistically, SAUR19s activate plasma membrane H^+-ATPases to induce apoplast acidification and cell expansion (Spartz *et al.*, 2014). We finally performed rhizosphere acidification assays. Seedlings were grown on B5 medium with normal or one-fifth iron concentrations for 7 d and then transferred to plates containing the pH sensor bromocresol purple

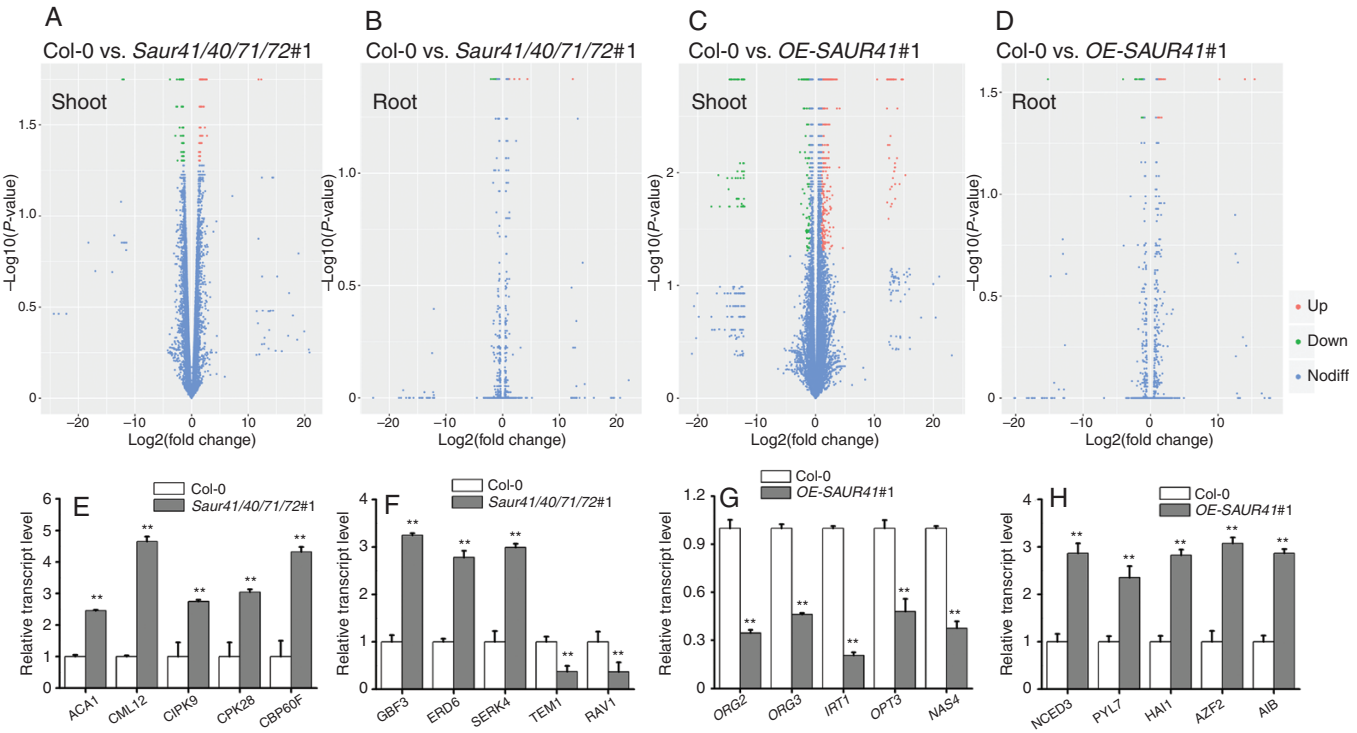

FIG. 6. Transcriptome profiling analysis of *saur41* quadruple mutants and *SAUR41* overexpression lines. (A–D) Venn diagrams illustrating differentially expressed genes in wild-type shoot vs. mutant shoot (A), wild-type root vs. mutant root (B), wild-type shoot vs. overexpression shoot (C) and wild-type root vs. overexpression root (D). Shoot samples had far more differentially expressed genes than root samples. (E–H) In 5-day-old seedlings, qRT-PCR validation of differentially expressed genes identified by transcriptome analysis. For each gene, the expression level in Col-0 was set to 1.0. (E) In the shoots of *saur41/40/71/72*, a set of calcium homeostasis/signalling genes are upregulated. (F) A set of ABA signalling-related genes are differentially expressed in the shoos of the quadruple mutants. (G) Overexpression of *SAUR41* decreases the transcription of iron homeostasis genes in roots. (H) Overexpression of *SAUR41* increases the transcription of ABA biosynthesis/signalling genes in shoots. Each treatment contained three biological replicates. Error bars represent the s.d. $^{**}P < 0.01$, $^{*}P < 0.05$, Student's *t*-test.

for 2 d. Extensive medium acidification was observed for the roots of *OE-SAUR41*, especially when the seedlings were from the one-fifth iron concentration medium (Fig. 9). In addition, overexpression of other members of the *SAUR41* subfamily, including *SAUR40, SAUR71* and *SAUR72*, also led to increased rhizosphere acidification (Supplementary data Fig. S7).

DISCUSSION

Data mining on arabidopsis transcriptional profiles revealed that the *SAUR41* subfamily genes are strikingly induced by the growth-inhibiting hormone ABA (Kodaira *et al.*, 2011; reviewed in Ren and Gray, 2015). Using qRT-PCR assay, we found that the expression patterns of *SAUR41* genes in arabidopsis seedlings were both overlapping and differential (Fig. 1). We verified that the transcription of *SAUR41* genes was induced by ABA, but not by GA and BR (Fig. 2; Supplementary data Fig. S2), in contrast to most other arabidopsis *SAUR* genes, which are repressed by ABA and activated by GA and BR (Kodaira *et al.*, 2011; reviewed in Ren and Gray, 2015). Thus, understanding the physiological roles of *SAUR41* genes seems promising to identify new players in plant ABA pathways.

The protein sequences of SAUR41s are highly conserved within the subfamily but show significant divergence from other SAURs, largely in the N-terminus (Kong *et al.*, 2013). Overexpression of *SAUR41* genes led to cell expansion-related phenotypes (Kong *et al.*, 2013; Qiu *et al.*, 2013). Among the 79 SAURs of arabidopsis, approx. 20 have been overexpressed and found to promote cell expansion in young seedlings (see the Introduction), regardless of their diverse subcellular localization. In contrast, knockout studies on arabidopsis *SAUR* genes are less documented, but have begun to be carried out in recent years (van Mourik *et al.*, 2017; Dong *et al.*, 2019). Here, using the CRISPR/Cas9 genome editing technique developed recently, loss-of-function mutants were generated for the *SAUR41* subfamily (Fig. 3), and some developmental and physiological phenotypes of quadruple mutants together with those of overexpression lines were characterized further (Figs 4–9). In those quadruple mutant seedlings, the lengths of hypocotyls, roots and cotyledon petioles and the areas of cotyledons were significantly reduced (Fig. 4; Supplementary data Fig. S4). In addition, thin and ultra-thin sections revealed that both in the quadruple mutants and in the *SAUR41* overexpression lines, there existed irregular arrangements of cell size and cell shape in hypocotyl pericycles and endodermis (Fig. 5). Thus, based on both loss-of-function and gain-of-function investigations, we conclude that SAUR41s are positive regulators of cell expansion, similar to the other arabidopsis SAURs investigated in recent years, including SAUR19s (Franklin *et al.*, 2011; Spartz *et al.*, 2012), SAUR63s (Chae *et al.*, 2012), SAUR36 (Stamm and Kumar, 2013), SAUR76–78 (Li *et al.*, 2015), SAUR14/50/65 (Sun *et al.*, 2016) and SAUR10s (van Mourik

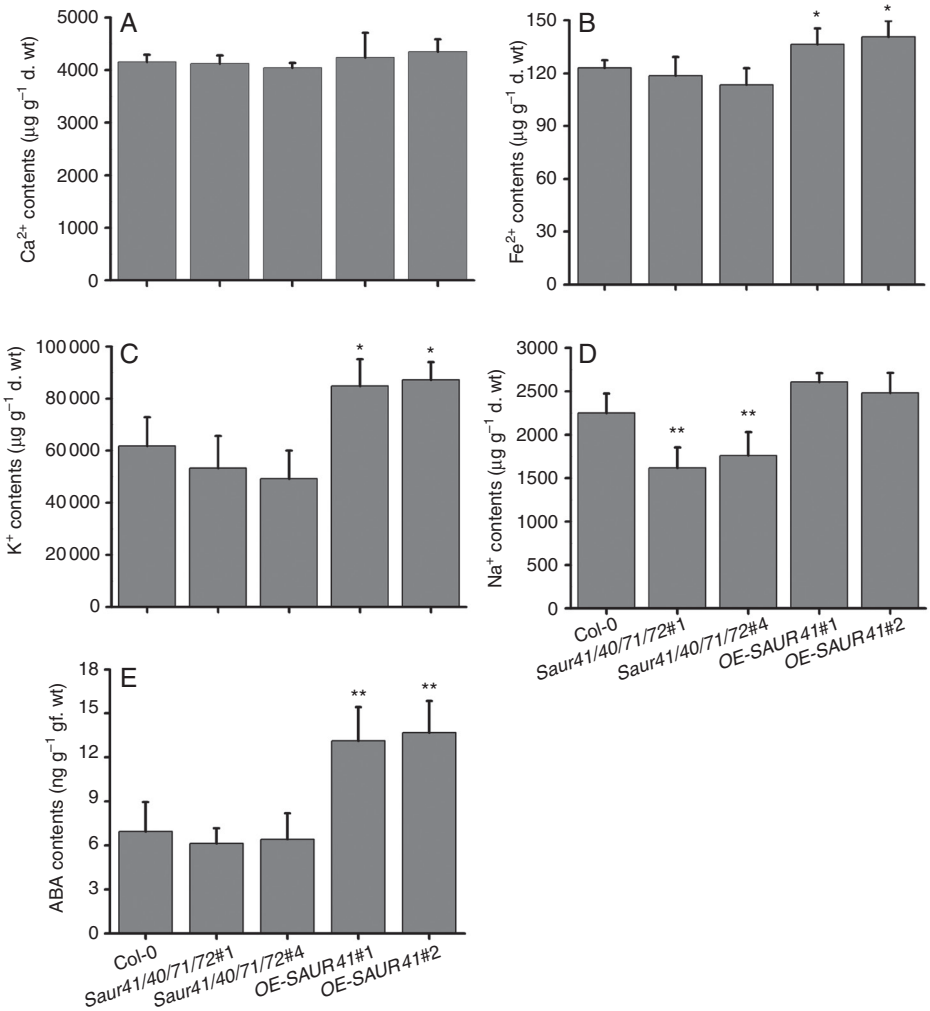

FIG. 7. Measurement of metal ion and ABA contents in 7-day-old seedling shoots. (A) There are no difference in calcium content among Col-0, *saur41/40/71/72* and *OE-SAUR41*. (B) The *SAUR41* overexpression lines have the highest levels of iron. (C) The *SAUR41* overexpression lines accumulate much more potassium. (D) The *saur41/40/71/72* mutants contain the lowest levels of sodium. (E) The *SAUR41* overexpression lines have 2-fold increased ABA contents as compared with the wild type. Each treatment contained three biological replicates. Error bars represent the s.d. $^{**}P < 0.01$, $^{*}P < 0.05$, Student's *t*-test.

et al., 2017). Because these SAURs span three clades and exhibit divergent expression patterns, the cell expansion promotion function of these proteins should be related to or attributed to the highly conserved approx. 60 amino acid SAUR domain.

Transcriptome analysis demonstrated that, in the shoot parts of the quadruple mutants, the Ca^{2+} homeostasis gene *ACA1* and certain Ca^{2+} signalling genes (*CML12/TCH3*, *CIPK9*, *CPK28* and *CBF60F*) were upregulated (Fig. 6E). Additionally, *GBF3*, a transcription factor gene responsive to ABA, water deprivation and bud dormancy (Gonzalez-Grandio *et al.*, 2017; Ramegowda *et al.*, 2017), was also upregulated (Fig. 6F). CIPK9 is a CBL-interacting protein kinase that regulates potassium homeostasis under low potassium stress (Pandey *et al.*, 2007; Liu *et al.*, 2013). Calcium signalling is crucial for regulating ion homeostasis in plant stress responses to cell wall integrity, salt, K^+ and pH (reviewed in Manishankar *et al.*, 2018), and the integration of ABA and calcium signalling is essential for evoking substantial cellular responses to various stresses (reviewed in Edel and Kudla, 2016). Interestingly, most arabidopsis SAUR proteins, including SAUR71 and SAUR72, contain a potential calmodulin-binding motif, although no functional significance has been ascribed to this motif to date (reviewed in Ren and Gray, 2015).

In seedling shoots of the *SAUR41* overexpression lines, the key ABA biosynthesis gene *NCED3* was up-regulated (Fig. 6H), and ABA content was increased (Fig. 7E). As reported, the transcription of *NCED3* is remarkably sensitive to the fluctuation of cell turgor (Sussmilch *et al.*, 2017). Thus, it is likely that accelerated and premature cell expansion reduced the hydrostatic pressure of cells overexpressing *SAUR41*, thus inducing ABA biosynthesis. Alternatively, SAUR proteins have unknown pathways to induce ABA biosynthesis. Although the *SAUR41* overexpression seedlings contained more ABA, these seedlings still exhibited increased cell expansion (Fig. 4; Supplementary data Fig. S4) and much higher potassium contents (Fig. 7C). These results may indicate that cell expansion

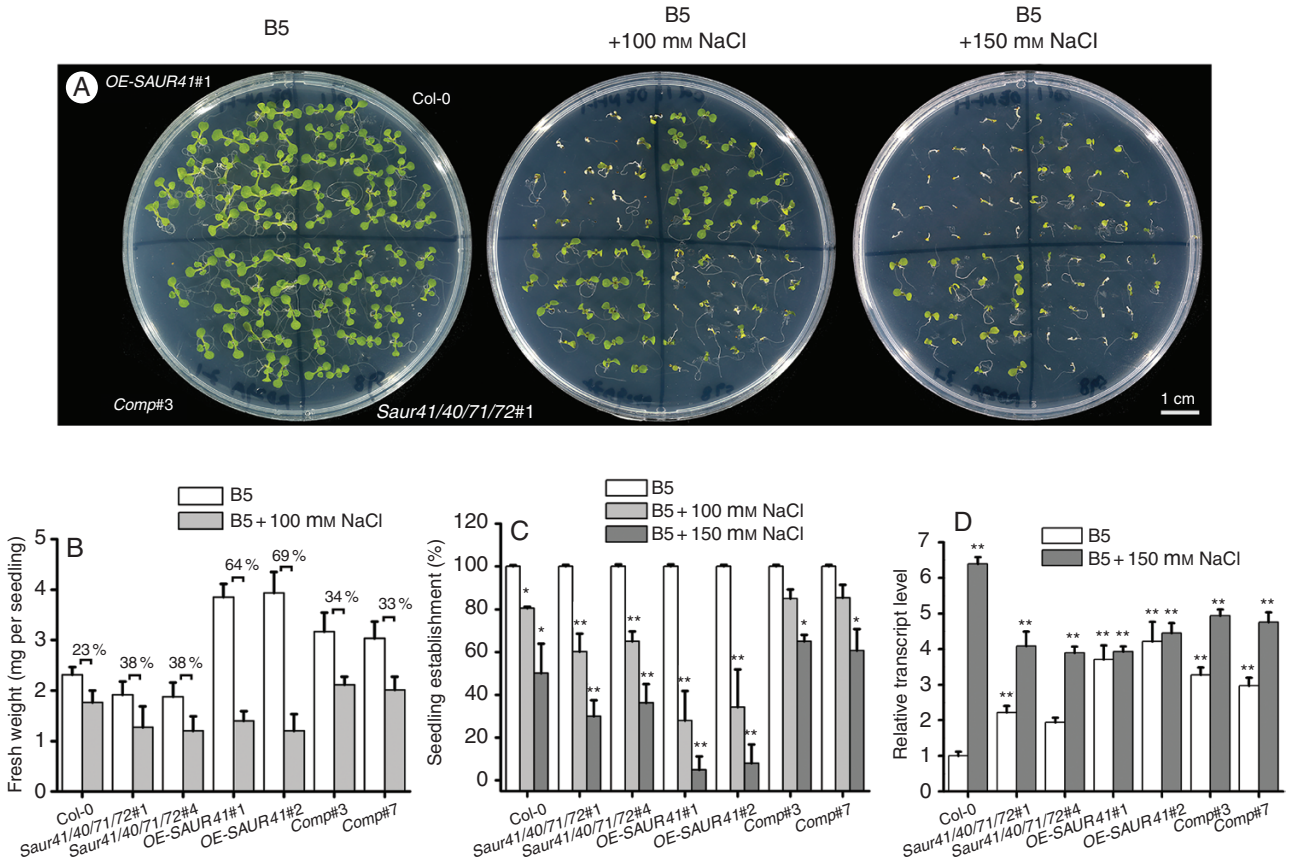

FIG. 8. Both the quadruple mutants and the *SAUR41* overexpression lines were hypersensitive to salt stress. (A) Seedling establishment and growth of the wild-type Col-0, quadruple mutants *saur41/40/71/72*, the *SAUR41* overexpression *OE-SAUR41* lines and the complementary lines Comp, grown on B5 media containing 100 or 150 mM NaCl for 7 d. The Comp lines were generated by specific expression of *SAUR41-EGFP* under the *RD29A* promoter (*proRD29A::SAUR41-EGFP*) in the quadruple mutant *saur41/40/71/72*#1. (B) Fresh weight of 7-day-old seedlings of four genotypes under salt stress. The labelled percentages are the rate of reduction of the fresh weight under salt stress. (C) Statistical comparison of percentage seedling establishment of four genotypes under salt stress. All the control treatments for the various lines had a 100 % seedling establishment rate. (D) qRT-PCR assay of the accumulation of *SOS1* encoding an Na^+/H^+ antiporter and a salt tolerance determinant. Each treatment contained approx. 30 seedlings or approx. 90 seeds and was replicated three times. Error bars represent the s.d. $^{**}P < 0.01$, $^{*}P < 0.05$, Student's *t*-test.

induced by ectopic SAUR41 is epistatic to the putative inhibitory effects of ABA on cell expansion.

The *SAUR41* overexpression lines were most sensitive to salt stress, whereas the quadruple mutants were moderately sensitive to salt stress (Fig. 8), indicating that a suitable expression level of *SAUR41* genes is required for arabidopsis salt tolerance. Supporting this notion, context-dependent expression of *SAUR41* under the ABA-responsive *RD29A* promoter in the quadruple mutants rescued the inhibitory effect of salt stress on seedling establishment (Fig. 8A–C). The *RD29A* promoter of arabidopsis contains two types of *cis*-acting elements for rapid (approx. 20 min) and slow (approx, 3 h) induction of gene expression under conditions of drought, high salt or low temperature (Yamaguchi-Shinozaki and Shinozaki, 1993, 1994). To improve plant stress tolerance, use of the strong constitutive *35S* promoter resulted in severe side effects under normal growth conditions, whereas use of the stress-inducible *RD29A* promoter eliminated the side effects and provided an even greater tolerance than the *35S* promoter (Kasuga *et al.*, 1999).

Three lines of evidence may explain why the *SAUR41* overexpression lines were those most unable to cope with salt stress. First, as reported, downregulation of most of the arabidopsis *SAUR* genes is involved in the inhibition of plant growth under salt stress (Kodaira *et al.*, 2011). Constitutive expression of *SAUR41* under a strong promoter (*35S*) may disturb the establishment of growth adaption under salt stress. Secondly, the *SAUR41* overexpression lines failed to increase the expression of *SOS1* under salt stress (Fig. 8D); enhanced expression of *SOS1* is a key determinant of salt tolerance (Shi *et al.*, 2000). Thirdly, overexpression of *SAUR41* led to disordered cell size and shape in the endodermis (Fig. 5), and this may disrupt the functional relationship between root/hypocotyl/leaf anatomy and salt tolerance (reviewed in Munns and Tester, 2008). As regards the quadruple mutants, they were able to increase the expression of *SOS1* under salt stress (Fig. 8D), and they contained the lowest contents of sodium under normal conditions (Fig. 7D), but they still displayed some weaknesses in salt tolerance (Fig. 8A–C). This could be explained in two ways. The quadruple mutants have the *SAUR41* subfamily genes knocked out, so they have reduced cell expansion in cells expressing *SAUR41* genes, which may lead to overinhibition under salt stress. In addition, they have disordered cell size and shape in the endodermis (Fig. 5).

The mechanisms whereby SAURs mediate cell expansion remain largely unknown. As reported, SAUR19s are thought to

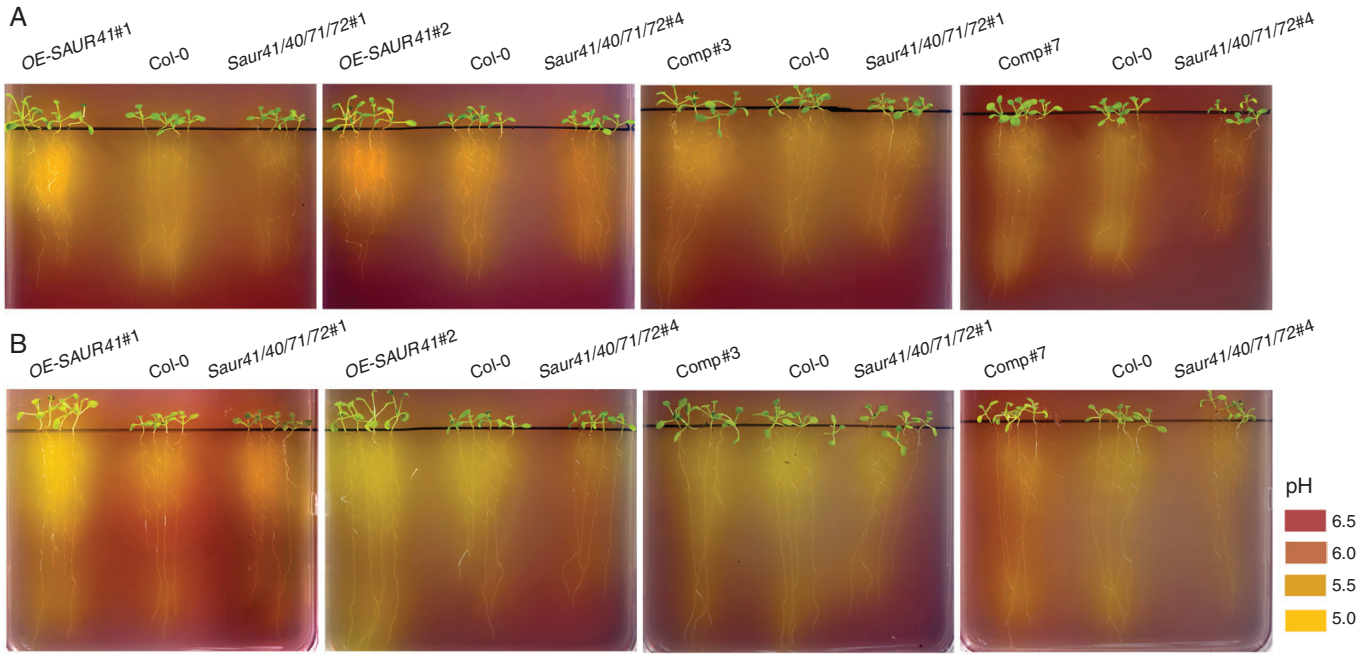

FIG. 9. Overexpression of SAUR41 led to extensive rhizosphere acidification. Seedlings were grown on B5 medium with normal (A) or one-fifth (B) iron concentrations for 7 d and then transferred to B5 plates containing the pH sensor bromocresol purple (0.003 %) for 2 d. Extensive medium acidification was observed for the roots of *OE-SAUR41*, especially when the seedlings were from the one-fifth iron concentration medium. A pH colorimetric panel is illustrated.

inhibit PP2C.D-type protein phosphatases to activate plasma membrane H^+-ATPases and to induce apoplast acidification (Spartz *et al.*, 2014). Similarly, it was found that SAUR40 and SAUR72 also inhibit PP2C.D1 in an *in vitro* phosphatase assay (Spartz *et al.*, 2014). Plasma membrane H^+-ATPases are powerhouses for plant physiology in regulation of cell expansion, solute uptake, phloem loading and tip growth (Palmgren 2001; Haruta *et al.*, 2015; Falhof *et al.*, 2016; Mangano *et al.*, 2018). It has been suggested that arabidopsis roots cope with iron deficiency by promoting plasma membrane H^+-ATPase 2 (AHA2)-mediated H^+ release into the rhizosphere to enhance the dissolution of Fe^{3+} (reviewed in Jeong *et al.*, 2017; Tsai and Schmidt, 2017). We found that overexpression of *SAUR41* led to increased acidification of the medium (Fig. 9) and increased iron contents (Fig. 7B), which may be responsible for the reduced transcription of iron absorption and transport genes because of extensive bioavailability of iron (Fig. 6). Therefore, it is rational to assume that SAUR41s may inhibit PP2C.Ds to activate plasma membrane H^+-ATPases. SAUR19s are peripheral membrane proteins, whereas SAUR41s are basically cytosolic proteins (Kong *et al.*, 2013; Qiu *et al.*, 2013). Nevertheless, the PP2C.D-type protein phosphatases are diverse in subcellular location, and different SAURs may have different PP2C.D partners (Ren *et al.*, 2018; discussed in Stortenbeker and Bemer, 2018).

Taken together, we propose that besides the ABA-repressed *SAUR* genes (Kodaira *et al.*, 2011), there exist ABA-induced *SAUR* genes (this study). Balanced expression of two types of *SAUR* genes may be necessary for salt tolerance. We suggest a working model for *SAUR41* genes in which ABA induces the expression of *SAUR41* genes to fine-tune seedling establishment and salt tolerance by modulating cell expansion and ion homeostasis (Fig. 10). Further investigation is needed to

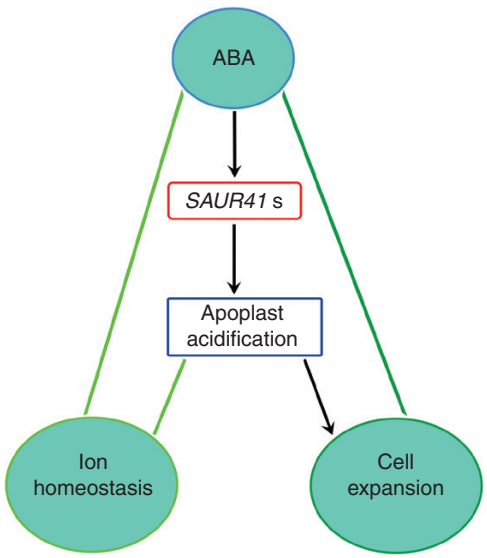

FIG. 10. A working model for the function of *SAUR41* genes. ABA induces the expression of *SAUR41* genes to fine-tune seedling establishment and salt tolerance by modulating cell expansion and ion homeostasis.

elucidate how the *SAUR41* pathway interacts with the core ABA signalling pathways and how a plant cell can distinguish extracellular acidification required for ion transportation and cell expansion. In addition, further examination of cell size in single, double and triple mutants would help to reveal distinctive and/or overlapping roles of individual members of *SAUR41* genes for cell size control. Considering that *SAUR41* genes are ABA inducible and ABA is a key hormone in plant abiotic stress signalling, our work may provide new candidate genes for improvement of plant abiotic stress tolerance.

SUPPLEMENTARY DATA

Supplementary data are available online at https://academic.oup.com/aob and consist of the following. Table S1: primer sequences used in the present study. Table S2: genes differentially expressed in root parts of the *saur41* quadruple mutants. Table S3: genes differentially expressed in shoot parts of the *saur41* quadruple mutants. Table S4: genes differentially expressed in root parts of the *35S::SAUR41-MYC* seedlings. Table S5: genes differentially expressed in shoot parts of the *35S::SAUR41-MYC* seedlings. Fig. S1: the design of guide RNAs targeting the coding sequences of *SAUR41* genes for the CRISPR/Cas9 genome editing. Fig. S2: BR response of *SAUR41* genes in 5-day-old arabidopsis seedlings as revealed by qRT-PCR. Fig. S3: predicted effects of each mutation on the corresponding protein product of *SAUR41* genes. Fig. S4: cotyledon petiole lengths in single, double, triple and quadruple mutants of *SAUR41* genes. Fig. S5: histograms for GO analysis of transcription profiling of the *saur41* quadruple mutants. Fig. S6: histograms for GO analysis of transcription profiling of the *SAUR41* overexpression lines. Fig. S7: overexpression of other *SAUR41* genes increased medium acidification in arabidopsis rhizosphere.

FUNDING

This work was supported by the Fundamental Research Funds for the Central Universities (no. 2017QNA6003), the National Program on Key Basic Research Project (no. 2014CB541704) and the Natural Science Foundation of Zhejiang Province (no. LY18C020001).

ACKNOWLEDGEMENTS

We thank Dr Holger Puchta (Karlsruhe Institute of Technology, Germany) for the CRISPR/Cas9 vectors, and VIB-Ghent University for plant GATEWAY™ destination vectors.

LITERATURE CITED

Arsuffi G, Braybrook SA. 2017. Acid growth: an ongoing trip. *Journal of Experimental Botany* **69**: 137–146.

Bechtold N. 1993. *In planta Agrobacterium*-mediated gene transfer by infiltration of adult *Arabidopsis thaliana* plants. *Compte Rendu de l'Academie des Sciences Paris, Sciences de la Vie* **316**: 1194–1199.

Bemer M, van Mourik H, Muino JM, Ferrandiz C, Kaufmann K, Angenent GC. 2017. Fruitfull controls *SAUR10* expression and regulates Arabidopsis growth and architecture. *Journal of Experimental Botany* **68**: 3391–3403.

Chae K, Isaacs CG, Reeves PH, *et al.* 2012. Arabidopsis *SMALL AUXIN UP RNA63* promotes hypocotyl and stamen filament elongation. *The Plant Journal* **71**: 684–697.

Cutler SR, Rodriguez PL, Finkelstein RR. 2010. Abscisic acid: emergence of a core signaling network. *Annual Review of Plant Biology* **61**: 651–679.

Deinlein U, Strphan AB, Horie T, Luo W, Xu G, Schroeder JI. 2014. Plant salt-tolerance mechanisms. *Trends in Plant Science* **19**: 371–379.

Dong J, Sun N, Yang J, *et al.* 2019. TCP4 and PIF3 antagonistically regulate organ-specific light induction of *SAUR* genes to modulate cotyledon opening during de-etiolation in Arabidopsis. *The Plant Cell* **31**: 1155–1170.

Edel KH, Kudla J. 2016. Integration of calcium and ABA signaling. *Current Opinion in Plant Biology* **33**: 83–91.

Engler C, Gruetzner R, Kandzia R, Marillonnet S. 2009. Golden Gate shuffling: a one-pot DNA shuffling method based on type IIs restriction enzymes. *PLoS One* **4**: e5553. doi: 10.1371/journal.pone.0005553.

Falhof J, Pedersen JT, Fuglsang AT, Palmgren M. 2016. Plasma membrane H^+-ATPase regulation in the center of plant physiology. *Molecular Plant* **9**: 323–337.

Fauser F, Schiml S, Puchta H. 2014. Both CRISPR/Cas-based nucleases and nickases can be used efficiently for genome engineering in *Arabidopsis thaliana*. *The Plant Journal* **79**: 348–359.

Favero DS, Le KN, Neff MM. 2017. Brassinosteroid signaling converges with Suppressor of Phytochrome B4-#3 to influence the expression of *SMALL AUXIN UP RNA* genes and hypocotyl growth. *The Plant Journal* **89**: 1133–1145.

Feng CZ, Chen Y, Wang C, Kong YH, Wu WH, Chen YF. 2014. Arabidopsis RAV1 transcription factor, phosphorylated by SnRK2 kinases, regulates the expression of ABI3, ABI4, and ABI5 during seed germination and early seedling development. *The Plant Journal* **80**: 654–668.

Franklin KA, Lee SH, Patel D, Kumar SV, *et al.* 2011. PHYTOCHROME-INTERACTING FACTOR 4 (PIF4) regulates auxin biosynthesis at high temperature. *Proceedings of the National Academy of Sciences, USA* **108**: 20231–20235.

Gonzalez-Grandio E, Pajoro A, Franco-Zorrilla JM, Tarancon C, Immink RG, Cubas P. 2017. Abscisic acid signaling is controlled by a branched1/HD-ZIP I cascade in Arabidopsis axillary buds. *Proceedings of the National Academy of Sciences, USA* **114**: e245–e254.

Guo Y, Jiang Q, Hu Z, Sun X, Fan S, Zhang H. 2017. Function of the auxin-responsive gene *TaSAUR75* under salt and drought stress. *The Crop Journal* **6**: 181–190.

Hagen G, Guilfoyle T. 2002. Auxin responsive gene expression – genes, promoters and regulatory factor. *Plant Molecular Biology* **49**: 373–385.

Haruta M, Gray WM, Sussman MR. 2015. Regulation of the plasma membrane proton pump (H^+-ATPase) by phosphorylation. *Current Opinion in Plant Biology* **28**: 68–75.

Hauser F, Li Z, Waadt R, Schroeder JI. 2017. Snapshot: abscisic acid signaling. *Cell* **171**: 1708–1708.

He SL, Hsieh HL, Jauh GY. 2018. SMALL AUXIN UP RNA62/75 are required for the translation of transcripts essential for pollen tube growth. *Plant Physiology* **178**: 626–640.

Hou K, Wu W, Gan SS. 2013. *SAUR36*, a *SMALL AUXIN UP RNA* gene, is involved in the promotion of leaf senescence in Arabidopsis. *Plant Physiology* **161**: 1002–1009.

Hubbard KE, Nishimura N, Hitomi K, Getzoff ED, Schroeder JI. 2010. Early abscisic acid signal transduction mechanisms: newly discovered components and newly emerging questions. *Genes & Development* **24**: 1695–1708.

Jeong J, Merkovich A, Clyne M, Connolly EL. 2017. Directing iron transport in dicots: regulation of iron acquisition and translocation. *Current Opinion in Plant Biology* **39**: 106–113.

Kant S, Bi YM, Zhu T, Rothstein SJ. 2009. *SAUR39*, a *SMALL AUXIN-UP RNA* gene, acts as a negative regulator of auxin synthesis and transport in rice. *Plant Physiology* **151**: 691–701.

Karimi M, Inze D, Depicker A. 2002. Gateway™ vectors for *Agrobacterium*-mediated plant transformation. *Trends in Plant Science* **7**: 193–195.

Kasuga M, Liu Q, Miura S, Yamaguchi-Shinozaki K, Shinozaki K. 1999. Improving plant drought, salt, and freezing tolerance by gene transfer of a single stress-inducible transcription factor. *Nature Biotechnology* **17**: 287–291

Kodaira KS, Qin F, Tran LS, *et al.* 2011. Arabidopsis Cys2/His2 Zinc-Finger proteins AZF1 and AZF2 negatively regulate abscisic acid-repressive and auxin-inducible genes under abiotic stress conditions. *Plant Physiology* **157**: 742–756.

Kong Y, Zhu Y, Gao C, *et al.* 2013. Tissue-specific expression of *SMALL AUXIN UP RNA41* differentially regulates cell expansion and root meristem patterning in Arabidopsis. *Plant & Cell Physiology* **54**: 609–621.

Leonhardt N, Kwak JM, Robert N, Waner D, Leonhardt G, Schroeder JI. 2004. Microarray expression analyses of arabidopsis guard cells and isolation of a recessive abscisic acid hypersensitive protein phosphatase 2C mutant. *The Plant Cell* **16**: 596–615.

Li ZG, Chen HW, Li QT, *et al.* 2015. Three SAUR proteins *SAUR76*, *SAUR77* and *SAUR78* promote plant growth in Arabidopsis. *Scientific Reports* **5**: 12477. doi: 10.1038/srep12477

Liu LL, Ren HM, Chen LQ, Wang Y, Wu WH. 2013. A protein kinase, Calcineurin B-Like Protein-Interacting Protein Kinase9, interacts with

Calcium Sensor Calcineurin B-Like Protein3 and regulates potassium homeostasis under low-potassium stress in Arabidopsis. *Plant Physiology* **161**: 266–277.

Ma P, Chen X, Liu C, *et al.* 2017. MeSAUR1, encoded by a *SMALL AUXIN-UP RNA* gene, acts as a transcription regulator to positively regulate ADP-glucose pyrophosphorylase small subunit1A gene in Cassava. *Frontiers in Plant Science* **8**: 1315. doi: 10.3389/fpls.2017.01315.

Mangano S, Pacheco JM, Marino-Buslje C, Estevez JM. 2018. How does pH fit in with oscillating polar growth? *Trends in Plant Science* **23**: 479–489.

Manishankar P, Wang N, Koster P, Alatar AA, Kudla J. 2018. Calcium signaling during salt stress and in the regulation of ion homeostasis. *Journal of Experimental Botany* **69**: 4215–4226.

Markakis MN, Boron AK, Van Loock B, *et al.* 2013. Characterization of a SMALL AUXIN-UP RNA (SAUR)-like gene involved in *Arabidopsis thaliana* development. *PLoS One* **8**: e82596. doi: 10.1371/journal.pone.0082596

Meng X, Chen X, Mang H, *et al.* 2015. Differential function of Arabidopsis SERK family receptor-like kinases in stomatal patterning. *Current Biology* **25**: 2361–2372.

van Mourik H, van Dijk ADJ, Stortenbeker N, Angenent GC, Bemer M. 2017. Divergent regulation of Arabidopsis SAUR genes: a focus on the SAUR10-clade. *BMC Plant Biology* **17**: 245. doi: 10.1186/s12870-017-1210-4

Munns R, Tester M. 2008. Mechanisms of salinity tolerance. *Annual Review of Plant Biology* **59**: 651–681

Pan X, Welti R, Wang X. 2010. Quantitative analysis of major plant hormones in crude plant extracts by high-performance liquid chromatography–mass spectrometry. *Nature Protocols* **5**: 986–992.

Palmgren MG.2001. Plant plasma membrane H^+-ATPases: powerhouses for nutrient uptake. *Annual Review of Plant Biology* **52**: 817–845.

Pandey GK, Cheong YH, Kim BG, Grant JJ, Li L, Luan S. 2007. CIPK9: a calcium sensor-interacting protein kinase required for low-potassium tolerance in arabidopsis. *Cell Research* **17**: 411–421.

Qiu T, Chen Y, Li M, *et al.* 2013. The tissue-specific and developmentally regulated expression patterns of the *SAUR41* subfamily of *SMALL AUXIN UP RNA* genes: potential implications. *Plant Signaling & Behavior* **8**: e25283.

Ramegowda V, Gill US, Sivalingam PN, *et al.* 2017. GBF3 transcription factor imparts drought tolerance in *Arabidopsis thaliana*. *Scientific Reports* **7**: 9148. doi: 10.1038/s41598-017-09542-1

Ren H, Gray WM. 2015. SAUR proteins as effectors of hormonal and environmental signals in plant growth. *Molecular Plant* **8**: 1153–1164.

Ren H, Park MY, Spartz AK, Wong JH, Gray WM. 2018. A subset of plasma membrane-localized PP2C.D phosphatases negatively regulate SAUR-mediated cell expansion in Arabidopsis. *PLoS Genetics* **14**: e1007455. doi: 10.1371/journal.pgen.1007455

She W, Lin W, Zhu Y, *et al.* 2010. The *Gypsy* insulator of *Drosophila melanogaster*, together with its binding protein Suppressor of Hairy-Wing, facilitate high and precise expression of transgenes in *Arabidopsis thaliana*. *Genetics* **185**: 1141–1150.

Shi H, Ishitani M, Kim C, Zhu JK. 2000. The *Arabidopsis thaliana* salt tolerance gene *SOS1* encodes a putativeNa^+/H^+ antiporter. *Proceedings of the National Academy of Sciences, USA* **97**: 6896–6901.

Shin JH, Mila I, Liu M, *et al.* 2018. The RIN-regulated Small Auxin-Up RNA SAUR 69 is involved in the unripe-to-ripe phase transition of tomato fruit via enhancement of the sensitivity to ethylene. *New Phytologist* **222**: 820–836

Spartz AK, Lee SH, Wenger JP, *et al.* 2012.The *SAUR19* subfamily of *SMALL AUXIN UP RNA* genes promote cell expansion. *The Plant Journal* **70**: 978–990.

Spartz AK, Ren H, Park MY, *et al.* 2014. SAUR inhibition of PP2C-D phosphatases activates plasma membrane H^+-ATPases to promote cell expansion in Arabidopsis. *The Plant Cell* **26**: 2129–2142.

Spartz AK, Lor VS, Ren H, *et al.* 2017. Constitutive expression of Arabidopsis *SMALL AUXIN UP RNA19* (*SAUR19*) in tomato confers auxin-independent hypocotyl elongation. *Plant Physiology* **173**: 1453–1462.

Stamm P, Kumar PP. 2013. Auxin and gibberellin responsive Arabidopsis *SMALL AUXIN UP RNA36* regulates hypocotyl elongation in the light. *Plant Cell Reports* **32**: 759–769.

Stortenbeker N, Bemer M. 2018. The SAUR gene family: the plant's toolbox for adaptation of growth and development. *Journal of Experimental Botany* **70**: 17–27

Sun N, Wang J, Gao Z, *et al.* 2016. Arabidopsis *SAURs* are critical for differential light regulation of the development of various organs. *Proceedings of the National Academy of Sciences, USA* **113**: 6071–6076.

Sussmilch FC, Brodribb TJ, McAdam SAM. 2017. Up-regulation of *NCED3* and ABA biosynthesis occur within minutes of a decrease in leaf turgor but AHK1 is not required. *Journal of Experimental Botany* **68**: 2913–2918.

Thomas JC, Sepahi M, Arendall B, Bohnert HJ. 1995. Enhancement of seed germination in high salinity by engineering mannitol expression in *Arabidopsis thaliana*. *Plant, Cell & Environment* **18**: 801–806.

Tsai HH, Schmidt W. 2017. Mobilization of iron by plant-borne coumarins. *Trends in Plant Science* **22**: 538–548.

Wild M, Daviere JM, Regnault T, *et al.* 2016. Tissue-specific regulation of gibberellin signaling fine-tunes Arabidopsis iron-deficiency responses. *Developmental Cell* **37**: 190–200.

Xu YX, Xiao MZ, Liu Y, Fu JL, He Y, Jiang DA. 2017. The *SMALL AUXIN-UP RNA OsSAUR45* affects auxin synthesis and transport in rice. *Plant Molecular Biology* **94**: 97–107.

Yamaguchi-Shinozaki K, Shinozaki K. 1993. Characterization of the expression of a desiccation responsive *rd29* gene of *Arabidopsis thaliana* and analysis of its promoter in transgenic plants. *Molecular and General Genetics* **236**: 331–340.

Yamaguchi-Shinozaki K, Shinozaki K. 1994. A novel cis-acting element in an Arabidopsis gene is involved in responsiveness to drought, low-temperature, or high-salt stress. *The Plant Cell* **6**: 251–264.

Yang Y, Jin H, Chen Y, *et al.* 2012. A chloroplast envelope membrane protein containing a putative LrgB domain related to the control of bacterial death and lysis is required for chloroplast development in *Arabidopsis thaliana*. *New Phytologist* **193**: 81–95.

Yuan Y, Wu H, Wang N, *et al.* 2008. FIT interacts with AtbHLH38 and AtbHLH39 in regulating iron uptake gene expression for iron homeostasis in Arabidopsis. *Cell Research* **18**: 385–397.

Zeng Y, Zhao T, Kermode AR. 2012. A conifer ABI3-interacting protein plays important roles during key transitions of the plant life cycle. *Plant Physiology* **161**: 179–195.